



Permafrost distribution and conditions at the headwalls of two receding glaciers (Schladminger and Hallstadt glaciers) in the Dachstein Massif, Northern Calcareous Alps, Austria

Matthias Rode¹, Harald Schnepfleitner¹, Oliver Sass², Andreas Kellerer-Pirklbauer¹ and Christoph Gitschthaler¹

5 ¹Department of Geography and Regional Science, Working Group on Alpine Landscape Dynamics (ALADYN), University of Graz

²Institute of Geography, Working Group on Geomorphology, University of Bayreuth

Correspondence to: A. Kellerer-Pirklbauer (andreas.kellerer@uni-graz.at)

10 **Abstract.** Permafrost distribution in rockwalls surrounding receding glaciers is an important factor for rock slope failure and rockwall retreat. The Northern Calcareous Alps of the Eastern European Alps form a geological and climatological transition zone between the Alpine Foreland and the Central Alps. Some of highest summits of this area are located in the Dachstein Massif (47°28'32"N, 13°36'23"E) in Austria reaching up to 2995 m a.s.l. Occurrence, thickness and thermal regime of permafrost at this partly glaciated mountain massif are scarcely known and related knowledge is primarily based on regional
15 modeling approaches. We applied a multi method approach with continuous ground surface and near-surface temperature monitoring, measurement of bottom temperature of the winter snow cover, electrical resistivity tomography/ ERT, airborne photogrammetry, topographic maps, visual observations and field mapping for permafrost assessment. Our research focused on steep rockwalls consisting of massive limestone above several receding glaciers exposed to different slope aspects at elevations between c.2600-2700 m a.s.l. We aimed to quantify distribution and conditions of bedrock permafrost particularly
20 at the transition zone between the present glacier surface and the adjacent rockwalls.

Low ground temperature data suggest that permafrost is mainly found at cold, north exposed rockwalls. At southeast exposed rockwalls permafrost is only expected in very favourable cold conditions at shadowed higher elevations (2700 m a.s.l.). ERT measurements reveal high resistivities (>30.000 ohm.m) at ≥1.5 m depth at north-exposed slopes (highest measured resistivity values > 100 kohm.m). Based on laboratory studies and additional measurements with small scale ERT, these values indicate
25 permafrost existence. Such permafrost bodies were found in the rockwalls at all measurement sites **independent of investigated slope orientation**. ERT data indicate large permafrost bodies at north exposed sites whereas discontinuous permafrost bodies prevail at northwest and northeast facing rockwalls. In summary, permafrost distribution and conditions around the headwalls of the glaciers of the Dachstein Massif is primarily restricted to the north exposed sector, whereas at the south exposed sector permafrost is restricted to the summit region.

30 **Keywords:** Dachstein, Eastern Alps, permafrost, electrical resistivity tomography, base temperature of the winter snow cover, ground surface temperature

1 Introduction

Climate change has a great impact on perennially frozen and glaciated high mountain regions (Haerberli and Hoelzle, 1995; Haerberli et al., 1997; Harris et al., 2001; Lieb et al., 2012). Glacier retreat (Paul et al., 2004; Zemp et al., 2006; Kellerer-
35 Pirklbauer et al., 2008) is the visible evidence with a loss of estimated 50% of the original glacier volume in the European Alps between the end of the Little Ice Age around 1850 and 1975, c.10% in 1975-2000 and further 10% in 2000-2009 (Haerberli et al., 2007, 2013, Magnin et al. 2017).



Invisible, but also measurable, are permafrost changes in the subsurface. **Once glacier-covered rock surfaces with former temperatures around the melting point – conditioned by temperate glacier ice – become subjected to direct local atmospheric conditions after the ice melted.** Depending on slope orientation and shading effects of these rock surfaces **permafrost aggradation is possible at such sites.** However, in case of cold and polythermal glaciers (with cold ice restricted to cold, high-altitude parts of the glacier; Benn and Evans, 2010) permafrost might exist even below glacier-covered areas. **In addition to that,** cirque glaciers are commonly separated from the headwall by a distinct crevasse (randkluft) separating the moving glacier from its headwall rock). Such a randkluft exists at several places in the study area (see Fig. 1) and is commonly visible during the ablation season. **The total length of the mapped randkluft in the area depicted in Fig. 1 is 2841 m, which is about 14.9 % of the total glacier boundary in this map. Air can enter into this crevasse allowing a better coupling of the air and bedrock even below the glacier surfaces and more efficient cooling during the autumn season. Therefore, both a polythermal glacier and a glacier with a distinct randkluft might allow permafrost aggregation below the glacier surface.**

A warming of about 0.5 to 0.8°C **in the upper tens of meters of alpine permafrost between 2600 and 3400 m a.s.l. at the European alps in the last century (Harris et al., 2003)** affects the long term thermal behavior of rockwalls and rock glaciers. **Since 1850 a vertical mean rise of the lower limit of permafrost by about 1m/year was calculated (Frauenfelder, 2005).** Changes in ground thermal conditions, permafrost extent and hydrology are all **sensitive to predicted future climate change** (Gobiet et al., 2014). Such changes have the potential to intensify rock breakdown and can be responsible for rockwall instabilities (Wegmann et al., 1998; Sattler et al., 2011; Raveland and Deline, 2011; Kellerer-Pirklbauer et al., 2012; Krautblatter et al., 2013; Draebing et al., 2017a, b). **Furthermore, the presence of permafrost in the rock has been proven to intensify frost weathering with subsequent rock falls (Matsuoka and Murton, 2008; Krautblatter, et al., 2013).**

Therefore, acquiring knowledge on the permafrost distribution and freezing and thawing in the active layer (Supper et al., 2014) is important in high mountain areas particularly if infrastructure is potentially threatened (Kern et al. 2012). Ground surface and near-ground surface temperature measurements in rockwalls (e.g. Matsuoka and Sakai, 1999; Gruber et al., 2003; Kellerer-Pirklbauer, 2017), as well as deep borehole data in bedrock (Harris et al., 2003), provide valuable point information on rock temperature and thermal conditions of permafrost. Geophysical techniques enable the detection, monitoring and visualization of subsurface permafrost characteristics indirectly and non-invasively from the surface. Several authors used electrical resistivity tomography (ERT) for permafrost investigations in sediments (e.g. Kneisel et al., 2008; Hauck, 2001; Hauck et al., 2003; Marescot et al., 2003; Laxton and Coates, 2011; Rödder and Kneisel, 2012; Stiegler et al., 2014). In contrast, in rockwalls comparable measurements are relatively scarce (e.g. Krautblatter and Hauck, 2007; Hartmeyer et al., 2012; Magnin et al., 2015, Draebing et al. 2017a, b) and for rockwalls close above the present glacier surfaces (Supper et al., 2014), ERT data are widely missing. Accordingly, the aims of this study are to detect, delimit and characterize permafrost in the rockwalls surrounding the Schladminger and Hallstatt glaciers in the Dachstein area. Both glaciers have been subject to substantial mass loss and glacier surface lowering in the last decades. **However, the resulting question about permafrost aggradation or degradation around receding glaciers in a mid-latitude alpine environment can't be answered based on this one-time investigation. The aim of the study is to delineate the current distribution of permafrost in this area.**

2 Study Area

The Dachstein Massif with its highest peak, the Hoher Dachstein (2995m a.s.l.) located at 47°28'32"N and 13°36'23"E, are a mountain range in the Northern Calcareous Alps in Austria covering an area of about 400 km² (Fig. 1). The study area is characterized by steep rockwalls (e.g. Dachstein south wall with 850 m altitude difference within a vertical distance of some hundred meters) towering relatively flat plateaus and summits, presently receding glaciers and extensive touristic infrastructure



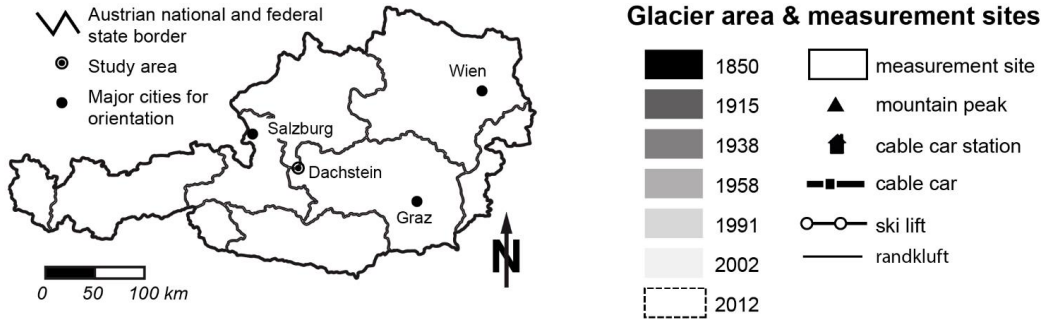
with cable cars, ski lifts and ski runs. The glaciers of the Dachstein Massif, in particular the Schladming Glacier (Fig. 1) is intensively used for alpine skiing. The surrounding headwalls are also partly used by means of a military transmitting station, lift stations and public climbing routes.

5 The prevailing rock type in the study area is the very compact Dachstein Limestone (GBA, 1982; Gasser et al., 2009). Our research focused on the lower parts of steep rockwalls at four different measurement sites (MS). These sites are located at the mountains Koppenkarstein (MS-K; summit elevation 2863 m a.s.l), Dirndln (MS-D; 2832 m a.s.l), Gjaidstein (MS-G; 2794 m a.s.l) and Hunerkogel (MS-H; 2687 m a.s.l) at elevations between 2600-2700 m a.s.l. (Fig. 1). These sites are located next to the Schladminger and Hallstatt glaciers.

10 The climatic conditions of the study area are dominated by west and northeast air flows. The main maximum of precipitation is during summer with a secondary maximum in winter. The Dachstein Massif is a climate divide with substantially lower precipitation at its south facing slopes compared to the north facing slopes at identical elevations (Wakonigg, 1978). Air temperature measurements at the surface of the Schladming Glacier next to the Hunerkogel at 2600 m a.s.l. showed annual average temperatures (MAAT) of -2.4°C from 2007-2016.

15 Glacier recession and surface lowering between the maximum glacier extent during the Little Ice Age/LIA (c.1850) and today changed the appearance of the landscape substantially. Hallstatt Glacier lost about 50% of its area and 52% of its length, whereas Schladming Glacier melted down by 55% (area) and 48% (length). The retreat of the glaciers located at the Dachstein Massif since the LIA are well documented by Simony (1895), Moser (1997), Krobath and Lieb (2004), Helfricht (2009) or Fischer et al. (2015). New ice-free areas in the glacier forefield and the surrounding head walls afforded new touristic concepts and safety precautions over the years, as for instance new secure climbing routes at the north face of the Koppenkarstein.

20 Scientific activities in the study area considering permafrost and rock falls have been scarce. The MAAT of -2.4°C (2007-2016) at about 2600 m a.s.l. at the Dachstein massif indicates the possible presence of discontinuous permafrost in the study area (Humlum, 1998). The first evidence of the existence of permafrost in the study area was provided by bottom temperature measurements of the snow cover (BTS) carried out by Schopper (1989) and Lieb and Schopper (1991) in the proglacial area of the Schladming glacier at 2300-2400 m a.s.l. According to these authors, the lower limit of discontinuous permafrost can
25 be expected at this elevation. More recent simulations regarding the probability of permafrost existence in Austria (Ebohon and Schrott, 2009) or in the entire European Alps (Boeckli et al., 2012 a, b) revealed that permafrost existence in the study area is particularly likely at north-exposed, higher elevated slopes as well as in the proglacial area of the Schladminger Glacier.



Extent of Fig. 2

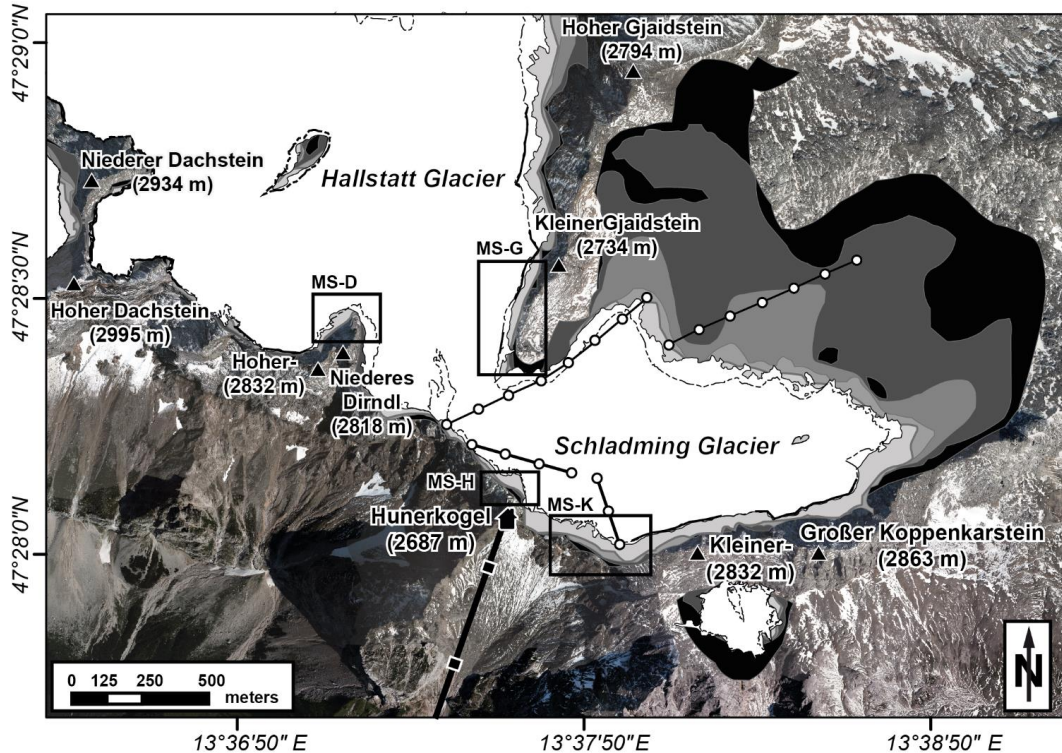


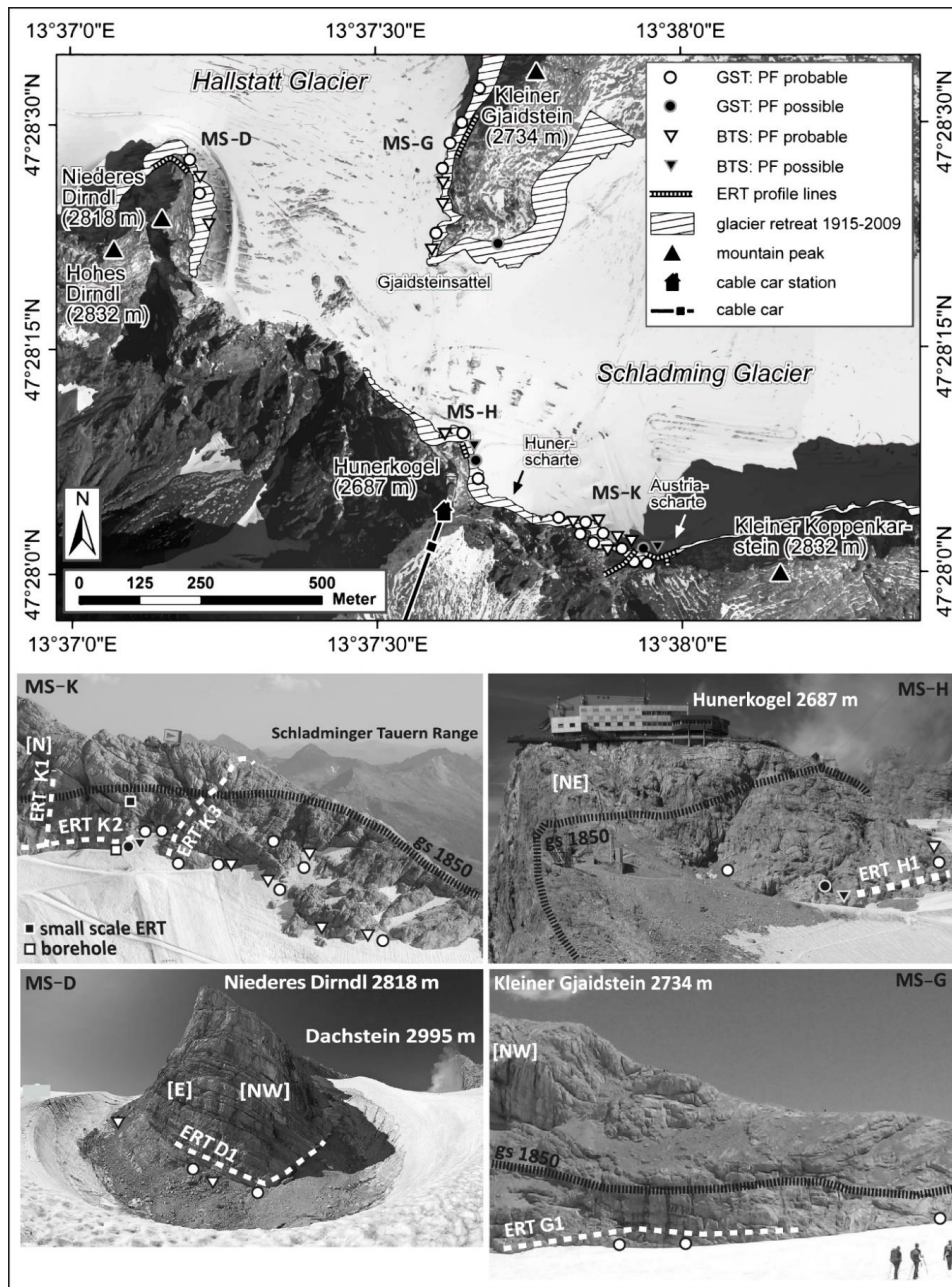
Figure 1: Location of the study area Dachstein Massif in Austria and an overview map depicting the four different measurement sites within the study area. Glacier recession between c.1850 (LIA maximum) and 2012 is indicated. Abbreviations: MS-D: measurement site Dirndl; MS-G: measurement site Gjaidstein; MS-H: measurement site Hunerkogel; MS-K: measurement site Koppenkarstein. Orthophoto in the background by Province of Upper Austria 2013.

3 Methods

A multidisciplinary approach was chosen to study the relationships between geology, glacier and permafrost in the study area. We used continuous ground surface temperature (GST) monitoring at the surface using miniature temperature datalogger, bottom temperature of the winter snow cover (BTS; Haerberli, 1973) and electrical resistivity tomography (ERT) profiling. The mentioned techniques have been used at all four measurement sites indicated in Fig. 1. Figure 2 shows all GST, BTS and ERT locations at the four measurement sites. Furthermore, a 7 m deep borehole was drilled into the north-facing rockwall of



Koppenkarstein in 2014 (Fig. 2; MS-K). Due to fragmentary data related to technical problems and hence missing continuous summer temperature data series no results are presented (Schnepfleitner et al. 2015). In addition, airborne photogrammetry, topographic maps, visual observations, field mapping and published glacier reconstructions (Simony, 1895; Moser, 1997; Krobath and Lieb, 2004; Helfricht, 2009; Fischer et al., 2015) were applied for the reconstruction of deglaciation.



5

Figure 2: Measurement locations of the different techniques at the studied rockwalls including interpretation of results of the GST and BTS measurements. The position of the glacier surface (gs) during the maximum of the LIA is indicated at all four sites. For details regarding interpretation of GST and BTS values see further below. Abbreviations: gs = glacier surface; PF = permafrost. Image data sources: Orthophoto by Province of Upper Austria 2013, terrestrial image of Niederer Dirndl by www.swisseduc.ch.



3.1 Base temperature of the winter snow cover (BTS)

BTS is based on the insulating properties of sufficiently thick snow cover (> 1 m), which prevents the ground surface from short-term periodical variations in air temperature (Haeberli, 1973, 1975). BTS is controlled by the heat flow of the subsurface and is distinctly lower above frozen ground. Haeberli (1973) defined temperatures < -3°C as permafrost areas, measurements
5 between -2°C and -3 °C as uncertainty range and temperatures > -2°C as non-permafrost areas. A self-constructed BTS thermocouple probe with a Pt100 (1/3 DIN class B) fixed to the bottom of a 3 m long steel rod (System KRONEIS, Vienna) at the lower end of a 3 m carbon tube was used. Measurements were performed at each point until constant temperature was registered for at least 2 minutes. The accuracy of measurements depends on several factors like calibration of the temperature sensor or disturbance of the temperature field by the breakthrough of the snow field by the probe. A total of 13 BTS-points (at
10 each point three measurements within an area of 2 m²; cf. Brenning et al., 2005) were determined at recently glacier free areas based on the multitemporal analyses of published maps and orthophotos (Fig. 2) in 2600 – 2700 m a.s.l. In the time period around the measurement date (20-03 to 21-03-2013), the snow cover recorded by a weather station at the Hunerkogel (snowreporter, 2013) increased continuously from 1.5 m (01-12-2012) to 3.5 m (25-03-2013). During the 13 BTS measurements snow depths ranged from 2 to 3.5 m. As pointed out by Brenning et al. (2005), BTS has to be interpreted as a
15 relative measure of ground thermal state and not strictly as a permafrost indicator.

3.2 Ground surface temperature (GST)

To avoid the restrictions of short BTS measurements, additional miniature temperature data loggers (iButtons, e.g. Gubler et al., 2011) were mounted at the bedrock surface. iButtons of type DS1922L, (Maxim Integrated) with a resolution of 0.5 °C and a measurement interval of 1 h were chosen. The sensors were placed in 20 very shallow boreholes with a depth of 2 cm
20 (Fig. 2). Additional protection against moisture was provided by small plastic bags. Preliminary laboratory calibrations of the sensors did not show any effects of the used plastic bags. iButtons were placed at the measurement sites at the rock surface beneath the snow pack on 01-01-2013 and removed on 31-07-2013. Therefore, up to 7 months of data were available for analysis.

With GST it is possible to monitor the seasonal temperature fluctuations at the uppermost centimeters of the surface (e.g.
25 Ishikawa, 2003). The winter equilibrium temperature (WEqT) describes temperature fluxes beneath the snow pack and is defined as the mean temperature of stable conditions during February and March. In case of strong temperature fluctuations – for instance related to atmospheric influence – during this period, the WEqT-approach is not applicable. As with BTS, strongly negative WEqT (< -3°C) are measured on frozen ground (permafrost areas) whereas on non-frozen bedrock the WEqT is usually close to 0°C or moderately negative. Another important parameter is the zero curtain period with temperatures around
30 0°C caused by the melting of the snow and isothermal conditions within the snow pack. The zero curtain period is framed by the basal-ripening date (RD), which describes the heating of the frozen ground by melting snow and the melt out date (MD), on which the snow cover is gone (Schmid et al., 2012).

3.3 ERT

For geophysical resistivity measurements, a constant current is applied into the ground through two 'current electrodes' and
35 the resulting voltage differences at two 'potential electrodes' are measured (Knödel et al., 2005). From the current and voltage values, an apparent resistivity value is calculated. ERT is excellently suited for permafrost detection as frozen ground is generally characterised by high electrical resistivity (due to the lack of conducting liquid water) and a strong contrast to the unfrozen surrounding (Hauck and Kneisel, 2008; Schrott and Sass, 2008). To determine the true subsurface resistivity in different zones or layers, an 'inversion' of the measured apparent resistivity must be carried out; we used the Res2Dinv



software package by Loke (1999). A GeoTom-2D system (Geolog2000, Starnberg, Germany) with multicore cables was used. Depending upon the local topography, between 24 and 50 electrodes were used. The connection between the electrodes and the rock was established by stainless steel screws, 12 mm in diameter, which were driven into 12 mm wide shallow boreholes, 50 mm deep and the spacing between two electrodes was 2 m. Thus, the total extent of the survey lines was between 32 and 5 98 m. Salt water and metallic grease were used to improve electrical contacts. Figure 2 shows the positions of the ERT measurements at rockwall MS-K, MS-H, MS-D and MS-G. The measurements were carried out by means of Wenner array which provides a particularly sound depth resolution in the central parts of the profile (Knödel et al., 2005; Loke, 1999). We used the robust inversion modelling process. The model discretization was set to use an extended model with an increase factor of model depth range of 1.5. Robust inversion delivered very good results in terms of low absolute error (maximum 15.5%).

10 To assess the quality of the results the depth of investigation (DOI) method was used (Oldenburg and Li, 1999; Hilbich et al., 2009; Stiegler et al., 2014). With this technique two inversions of the same data sets are carried out using equation (1), but with two different reference models with homogeneous resistivity values m_{01} and m_{02} (Hilbich et al., 2009). The first reference value (m_1) is usually calculated from the average of the logarithm of the observed apparent resistivity values. The second reference resistivity value (m_2) is usually set at 10 times this value. Model regions with DOI index values >0.2 are considered

15 as unreliable (Hilbich et al., 2009). This empirical method determines the effective depth of investigation (Angelopoulos et al., 2013).

$$DOI(x, y) = \frac{m_1(x, z) - m_2(x, z)}{(m_{01} - m_{02})}, \quad (1)$$

Inversion artefacts are often caused by high resistivities and high resistivity contrasts between frozen and unfrozen subsurfaces and can lead to misinterpretations of the inversion model tomograms. Applying synthetic modelling can be used to confirm the hypotheses drawn from the observed internal permafrost structure of the rockwall. By using the software Res2Dmod (Loke, 1999) simulated data of the expected apparent resistivities were calculated with the same measurement setup as in the field. 5 % Gaussian noise was added to the apparent resistivities to simulate field conditions (Hauck, 2001; Stiegler et al., 2014). The robust inverted synthetic model was compared to the real inverted data. The modelling process continued until both inverted data sets had similar tomograms. The final synthetic model was used as a possible representation of the subsurface (Hilbich et

25 al., 2009; Stiegler et al., 2014).

3.3.1 Resistivity category definition

To determine the thermal condition within the rockwall the resistivity values have to be grouped into different categories. In this study the results of a small-scale geoelectric monitoring station used for rock moisture and frost weathering research nearby to the ERT-profiles at the Koppenkarstein (Fig. 2, MS-K) were used to classify the resistivities. The same GeoTom-2D system with multicore cables for 68 electrodes was used. The connection to the rock was established by stainless steel screws, 5 mm in diameter, which were driven into 4 mm boreholes, 1 cm deep and 6 cm apart. Thus, the total extent of the survey line was 4.08 m. Additional temperature sensors (Pt1000, Geoprecision) at 0, 2, 6, 12 and 18 cm depth gave simultaneous information about the temperature behaviour within the rock. The combined analysis of resistivity and temperature changes at different depths caused by freeze thaw events provides the necessary information to define the rock resistivity characteristics at different temperatures. The mean resistivities along the whole profile at 2, 6, 12 and 18cm depth were compared with the temperature results. Similar to the laboratory results of Krautblatter et al. (2010), a rapid increase in resistivity from 13 kohm.m to 30 kohm.m was observed in the temperature range between -0.5 and -1°C (Fig. 3). The unfrozen rock was characterized by resistivities of up to 13 kohm.m, the transition zone with still unfrozen layers ranged from 13-30

35



kohm.m and frozen rock had resistivities exceeding 30 kohm.m. Similar thresholds were used by Krautblatter et al. (2007) and Magnin et al. (2017).

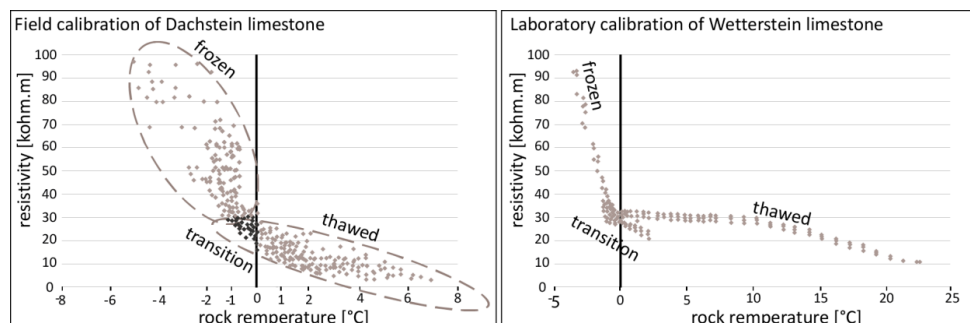


Figure 3: Comparison of small scale ERT (left) and laboratory (right; Krautblatter et al. 2010) calibration measurements.

5

3.4 Deglaciation reconstruction

To get more information about the vertical changes of the glacier surface and to visualize the ice free rockwalls, digital terrain models (DTM) with a spatial resolution of 5 m were produced from published 1:25,000 maps of the German-Austrian Alpine Society from 1915 and 2002. The two maps were scanned and the 10 m contour lines were digitized in ArcGIS 10.0 and DTMs were generated using the Topo-to-Raster function. The adequate quality of the calculated surfaces was confirmed by comparing the output data (contour lines of the calculated DTMs) with the input data (contour lines from the maps). The difference between both models finally showed the glacier retreat of 1915 to 2002. In addition, recent orthophotos from 2009 (provided by the Federal Government of Upper Austria) and data from the third Austrian glacier inventory (Fischer et al., 2015) enabled the mapping of the present glacier surface and so the estimation of the glacier retreat of 1915 to 2009. The comparison of historic photographs from 1958 (Schneider, July 1958 from Österreichischer Alpenverein 1958) and own photographs from 2013-2015 gave further information about the vertical surface lowering (Fig. 4). The poor quality and widespread existence of late-lying winter snow in some of the photographs hindered an exact comparison of all investigated rockwalls.

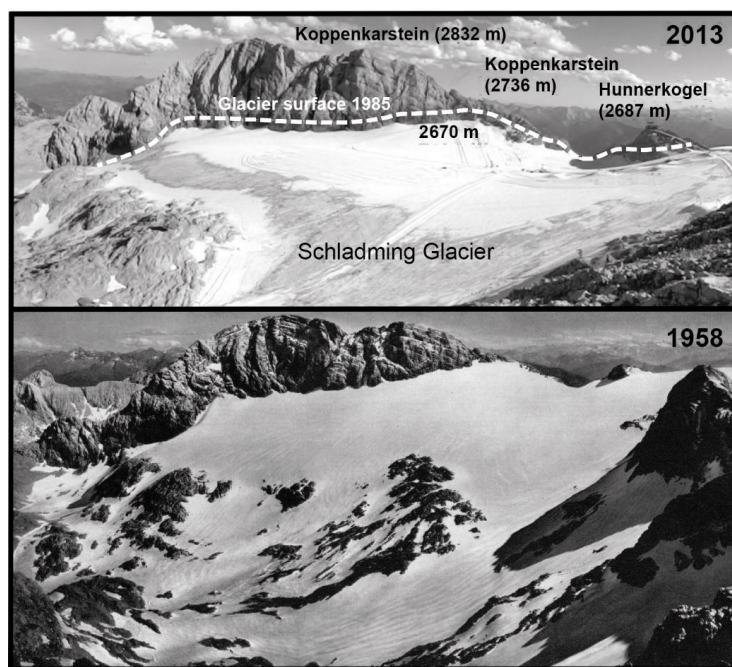


Figure 4: Comparison of the glacier surface at the foot of the Koppenkarstein in 2013 (photo Gitschthaler, 02-08-2013) and 1958 (photo Schneider, July 1958 from Österreichischer Alpenverein 1958). Note the obvious surface change at Hunerkogel. Note that the shooting location of both years is not exactly the same.

5 4 Results

4.1 BTS and GST

Figure 5 shows the results of the GST measurements, carried out at the sites MS-K, MS-H, MS-D and MS-G. Measurement locations including additional BTS points are shown in Fig. 2. The temperature curves from January to July 2013 display that the WEqT, as an indicator for permafrost, could be measured at all sites, as well as the zero curtain, RD and MD. At the north exposed MS-K the mean WEqT of nine GST measurements is -3.9°C , the mean of the six BTS measurements is -5.0°C . At 10 MS-H the WEqT (iB-H2) and BTS in northeast aspect is with -5.2°C resp. -5.6°C significantly lower than the measured values at the east exposed rockwall. There, the mean WEqT (iB-H1, iB-H3) is -3.1°C , the mean of the BTS values is even higher (-2.2°C , maximum value of all temperature measurements). At MS-D the mean WEqT of the two iButtons in northeast exposure is -3.6°C while the mean BTS, measured north exposed, is -4.2°C . For MS-G the results show some more fluctuation in 15 temperature at the beginning of the year (iB-G1, February), probably because of less insulation due to a shallow snowpack. The temperature values of iB-G1 but also of the adjacent BTS measurement at the south end of the ridge to Kleiner Gjaidstein are therefore lower than those of the surrounding measurements. Mean WEqT of all GST measurements carried out at the foot of the west to northwest exposed slope is -4.3°C , the mean BTS is -4.5°C . The WEqT of the southeast exposed iB-G2 is more than 1 K higher (-2.9°C), which can be explained by much higher direct solar radiation.

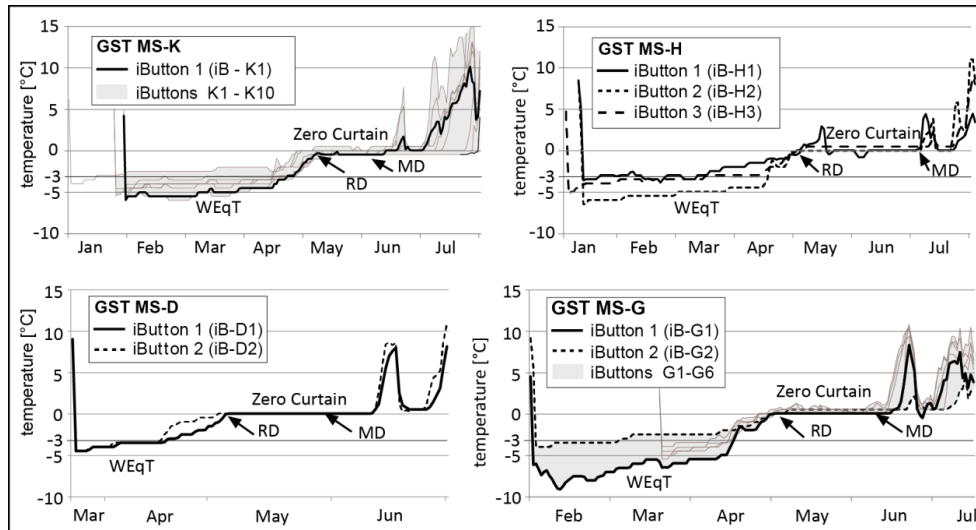


Figure 5: GST measurements from January 2013 to July 2013. Abbreviations: WEqT = winter equilibrium temperature; RD = basal-ripening date; MD = melt-out date.

4.2 ERT

- 5 The thermal resistivity classification from Fig. 3 constitutes the base for the interpretation of the ERT measurements at the four investigated rockwalls. Table 1 gives an overview of the 6 ERT profiles including interpreted permafrost existence.

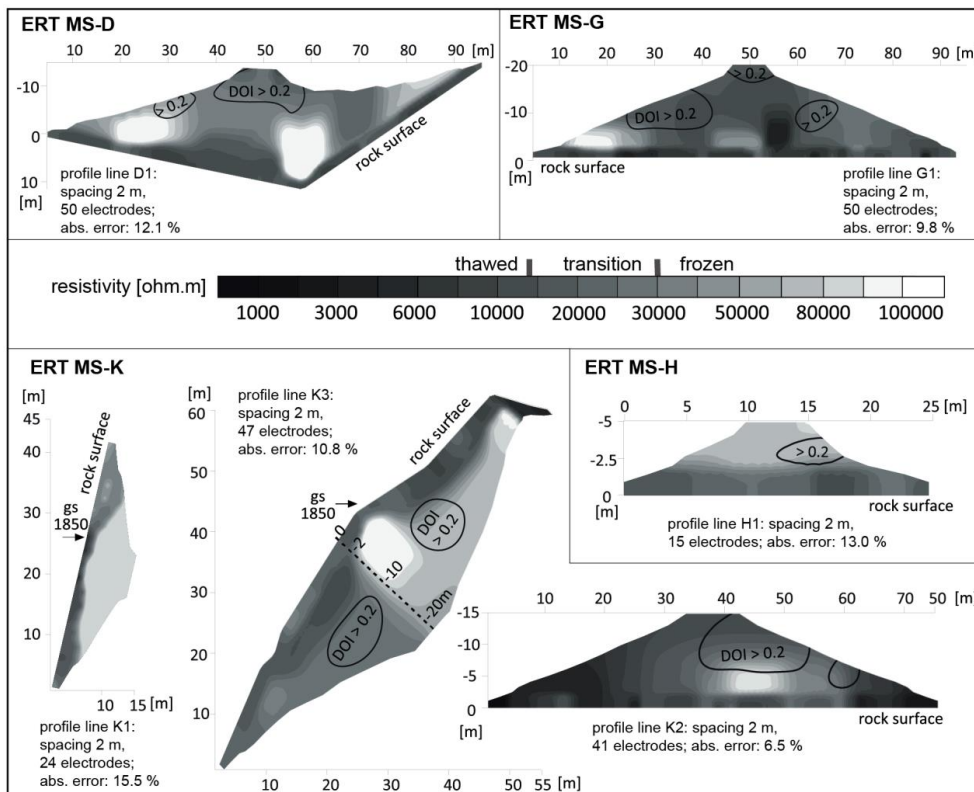
Table 1: ERT profiles information. Abbreviation: PF = permafrost.

MS + date 05.09.-09.09. 2013	code	elevation [m a.s.l.]	length [m]	alignment	resistivity [kohm.m]	PF
MS-K	ERT K1	2640 - 2680	48	vertical	7 - 500	yes
	ERT K2	2640	80	horizontal	4 - 330	yes
	ERT K3	2635 - 2700	92	vertical	5 - 300	yes
MS-H	ERT H1	2620	32	horizontal	9 - 160	yes
MS-D	ERT D1	2630	98	horizontal	7 - 300	yes
MS-G	ERT G1	2580	98	horizontal	4 - 300	yes

In Fig. 6 all ERT profiles use the same specific resistivity scaling delineating the three possible thermal conditions. At MS-D, high resistivities (> 30 kohm.m) are recognizable beneath 1.5 m depth. There are also two zones with resistivities of more than 100 kohm.m. At MS-G also layers with resistivities above 30 kohm.m were detected below 1 m depth. Compared to MS-D the resistivities are lower and more heterogeneous with only one zone of resistivities higher than 100 kohm.m near the east end of the profile. At MS-H, only a short ERT profile was possible because of numerous lightning rods installed at the rockwall for the protection of the lift station. Nevertheless, an increase of resistivity is observable with rock depth; beneath 2 m depth the resistivities are between 30 and 80 kohm.m. At the north face of MS-K three ERT profiles were installed, two of them in



vertical settings. These two profiles cross the line where the glacier surface was located during the LIA maximum. The resistivity distribution at ERT profile line K3 with a length of 92 m and a penetration depth of almost 20 m shows higher resistivities (>30 kohm.m) at the upper part and lower resistivities at the lower part (10 – 30 kohm.m). In the center of the profile line below 2 m depth, resistivities of more than 100 kohm.m were observed. Generally higher resistivities (from 20 to > 100 kohm.m) were measured at ERT profile line K1. Like ERT profile lines D1 and G1 ERT profile K2 was measured just above the present glacier surface. Like at the other three horizontal profiles, an extreme increase of resistivity (from 10 to more than 30 kohm.m.) towards depth is shown. The DOI indexes prove the reliability of all data sets to depths of about 10-15 m with zones having a smaller DOI index than 0.2 (Fig.6). The absolute error values of all inversions are between 6.5 % and 15.5 %.



10

Figure 6: ERT results at MS-D (measurement site Dirndln), MS-G (Gjaidstein), MS-K (Koppenkarstein) and MS-H (Hunerkogel). gs 1850 = glacier surface at c. 1850

To interpret the ERT measurement, important statistical values are shown in Fig. 7. The ERT-Profiles were divided into 1 m depth sections and the measured values were displayed in a box plot. Besides the profile ERT-MS-G, all other values of the recorded profiles are above 30 kohm.m. At the profile ERT-MS-D, values above 30 kohm.m were recorded at a depth of 1 to 2 m. Between 2 and 3 m, already 50% (Q2) of the data (also the mean) are above the 30 kohm.m limit. From a depth of 4 m, this limit reaches 70% (with increasing depth, this value still increases) of the measured data. Similar distributions, but with a smaller value range, can be found in profile ERT-MS-K3. The distribution of the measured data at the profiles ERT-MS-K1 and ERT-MS-K1 is even more substantial. From a depth of ≥ 2 m, 100% of the values are above the limit of 30 kohm.m. In the profile ERT-MS-K2, 50% of the values as well as the mean exceed the limit, already in the near-surface areas. From a depth of >7m 90% of the values pass the limit. Based on this statistical analysis the existence of permafrost could not be confirmed

20



at the measurement site ERT-MS-G. Although values above 30 kohm.m are reached, is the number of values ≥ 30 kohm.m too small for a significant statement. Overall, however, this evaluation confirms very well the results shown in Fig. 6.

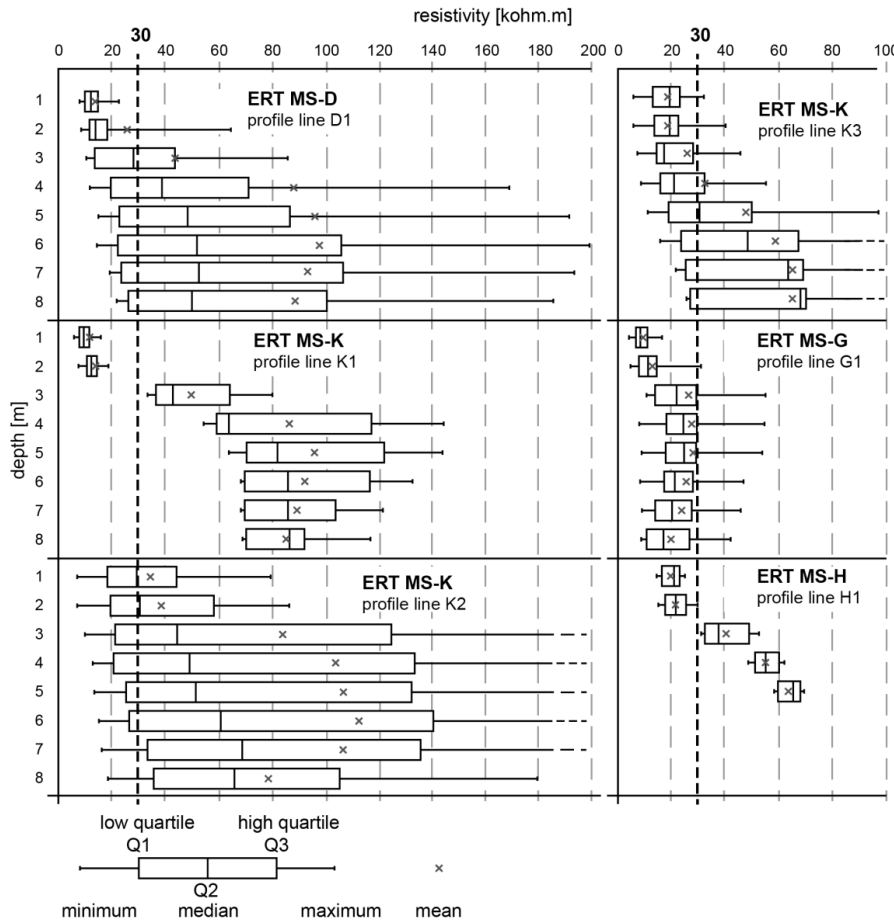


Figure 7: Boxplots of measured resistivity at depths from 0-8 m over the entire measuring profile. Value range for depth 1: $0 < \leq 1$ m; 2: $1 < \leq 2$ m and so on.

4.3 Deglaciation reconstruction

Table 2 shows the ascertained horizontal recession and vertical surface lowering rates of the glacier area between 1915 and 2009 for the four measurements sites (see also Fig. 2). For the MS-K the horizontal recession is about 20 m near the Austriascharte but only 5-10 m at the north face of the Koppenkarstein. The vertical loss there is about 15-20 m. Similar amounts of vertical decline can be estimated for the area around the Hunerkogel (MS-H) (cf. Fig. 4), the horizontal recession there amount to 15-30 m (at the Hunerscharte about 20m). For the MS-D the horizontal recession is about 20-50 m, vertically the glacier has lost 5-25 m with highest amounts in northwest exposition. Around the Gjaidstein (MS-G) maximum decline rates, both horizontal and vertical, can be determined. The horizontal decrease of ice at this site is highest at the south and southeast exposed areas of the Schladminger Glacier (up to 70 m), the vertical loss there is about 15-35 m. The vertical decrease west of the ridge from the peak of Gjaidstein to the Gjaidsteinsattel is up to 50 m, with highest losses northwest (up to 50 m) and west (up to 30 m) of the summit and lower values (only 5 m) getting closer to the Gjaidsteinsattel.



Table 2: Horizontal recession and vertical surface lowering rates of the glacier areas in the four sub-regions of interest (Fig. 1) between 1915 and 2009

Measurement site	MS-K	MS-H	MS-D	MS-G
Horizontal decline [m]	5-20	15-30	20-50	20-70
Vertical decline [m]	15-20	15-20	5-25	5-50

5 Discussion

5.1 Permafrost distribution

The permafrost model by Boeckli et al. (2012 a, b), which includes explanatory variables like annual air temperatures, potential incoming solar radiation and precipitation, fits quite well with our own field work results (Fig. 5-7). According to the GST/BTS classification defining temperatures < -3 °C as permafrost areas, measurements between -2 °C and -3 °C as uncertainty range and temperatures > -2 °C as non-permafrost areas (Haeberli, 1973), almost all areas are affected by permafrost in cold and permafrost in favorable conditions (Böckli et al., 2012a). Long time (2004-2015) GST measurements in permafrost at a nearby mountain (Hochreichart 2416 m a.s.l.) show a general increase of the mean annual ground temperature (Kellerer-Pirklbauer, 2016). The mean annual temperature of 2013 at the Hochreichart site was an average value for the entire 2014-2015 period suggesting that our ground temperature data of 2013 for the Dachstein might be regarded as typical not only for a single year but at least for a decadal time-scale. Especially at northerly oriented rockwalls, modelled and detected permafrost are in good coincidence. At all four study sites permafrost layers with resistivities higher than 30 kohm.m occurred. Highest resistivities were found at the MS-K north face, followed by the MS-D site, while at the MS-G and MS-H the resistivities were lower and the border to the permafrost layers are not so pronounced (Fig. 6). The GST results support this resistivity order, with deeper WEqT temperatures beneath -5 °C at MS-K (near the borehole) and WEqT between -5 and -3 °C at the three other sites. At MS-K, the thinnest active layer and the highest resistivities of the deeper subsurface were found in the approximate middle of the vertical profiles, corresponding with the 1850 glacier surface. This is particularly well visible at the K1 profile. The flattening of the rockwall at K3 in the elevation of the 1850 surface probably enabled accumulation of infiltrated moisture and the development of massive ice below the surface (-2 to -10 m). Generally higher resistivities (>50 kohm.m) were found in the part of the rockwall which has been ice-free during the last >150 years. At the ERT-sites near the present glacier surface (MS-K - K2, MS-D - D1, MS-G - G1 and MS-H - H1) which have been ice-free for a much shorter time, resistivities are lower and the active layer is thicker.

At D1 it is difficult to determine the historically highest surface of the glacier extent, because the glacier surface at the Dirndl mountain is highly influenced by wind causing snow-poor and ice-free conditions at the footslope of this mountain forming a distinct blowout depression between the glacier and the mountain (Fig. 2). The investigated part of the rockwall at D1 was probably ice free even before 1850 (Simony, 1884) and thus much longer exposed to atmospheric conditions than K2, G1 and H1. The absence of insulating glacier ice could be the reason for the well-established ice layers at the left and in the middle of the profile beneath the active layer. However, between those two frozen parts thawing processes occur with resistivities between 10 and 20 kohm.m, mirrored by a wet and fractured rock surface in the field. The situation at MS-H is of particular interest because it is heavily used by touristic infrastructure with a cable car station on the top. Originally, it was not expected to detect permafrost at this site because of the rather small and lower-elevated rock peak. Nevertheless, the results at H1 point



to permafrost which is also underpinned by the temperature measurements at least at the north-east exposed direction. However, at places like the Hunerkogel the Boeckli et al. (2012a) model assumes permafrost only in very favorable conditions. Our own results suggest that there is more permafrost than assumed which is important for further infrastructure projects. Conversely, in south east exposed rockwalls at the Dirndl and at the Gjaidstein permafrost is probable only in very favorable
5 conditions. The results broadly agree with Magnin et al. (2017) who have suggested that isolated permafrost bodies could exist down to 2800m at favorable S-exposed sites while in N-exposed locations, permafrost can also occur at significantly lower altitudes in the Montblanc massif.

5.2 Significance of ERT data for permafrost detection

The use of salt water and conductive grease at the drilled-in screws bypassed high contact resistances obtained between
10 electrodes and ground and provided satisfactory data quality. ERT permafrost investigations in bedrock are always error-prone. Whereas the resistivity contrast between ice and unfrozen water is huge, it is small between ice, air and certain rock types, as all three nearly behave as an electrical insulator with very high resistivities (Hauck and Kneisel, 2008). Furthermore, the resistivity values for subzero ground span a wide range from about 13 kohm.m to more than 30 kohm.m depending on the ice content (Hilbich et al., 2009). At all six ERT profile lines, areas with resistivities higher than 100 kohm.m up to 500 kohm.m
15 (Table 1) were measured which, in all probability, represent frozen ground. The usage of the DOI method showed, that mainly at high resistivity changes (between thawed and frozen layers) some areas with DOI > 0.2 were calculated and should be discussed with caution (Hilbich, 2009). On the whole, the DOI analyses showed that all ERT profiles are reliable and allow a detailed interpretation of the different resistivities.

20 To exclude resistivity misinterpretations, temperature-dependent resistivity determination by small scale geoelectric were performed (see Fig. 3). Laboratory calibration of temperature-resistivity relationship have to imitate natural conditions and the resistivities have to be calculated under the assumption of half-space geometry with deviations of current flow from real half space conditions (Krautblatter et al., 2010). The combined use of small scale ERT measurements and temperature sensors at different depths presented here gives - in contrast to lab approaches - the natural resistivity changes by freezing and thawing
25 down to depths of about 50 cm. Micro cracks and fissures along the profile and zones of different moisture saturation represent the natural rock conditions and are included in the resistivity calibration. The transition zone with a mixture of liquid water and ice with values between 13 and 30 kohm.m is characterized by the rapid increase of resistivity from 5 kohm.m to 10 kohm.m at the temperature change from positive to negative (starting around -0,5° C). During constant freezing and temperatures below -0.5 °C, values higher than 30 kohm.m. were measured. Krautblatter et al. (2010) also determined 30
30 kohm.m as an initial value for frozen Wetterstein limestone which is very similar to the Dachstein Limestone at the small scale ERT profile line (cf. Fig. 3).

5.3 Degradation or aggradation of permafrost?

Significant areas of the study region were affected by glacier recession and glacier surface lowering at the glacier forefield and
35 the surrounding headwalls. The thermal regimes of surface ice and frozen ground can be interconnected and are influencing each other (Suter et al., 2001; Otto and Keuschnig, 2014). The occurrence of permafrost in recently ice free rockwalls is proven by our results. An open question is if this permafrost has newly formed since glacier recession or if permafrost was already present under the ice?



At both vertical profiles K1 and K3 at MS-K (Fig. 6) the largest area and highest resistivities of frozen rock is present near the 1850 glacier ice surface line. Frozen rock at some meters rock depth below the 1850 glacier surface level might be due to permafrost aggradation due to the access of cold air since the beginning of glacier lowering. In this case, the glacier base should have been warm-based. However, in case the glaciers in our study area are polythermal (i.e. of type d. on Fig. 2.6. in Benn & Evans, 2010), permafrost might exist under the cold-based areas of glacier ice. In this case, the active layer which developed since deglaciation would indicate current permafrost degradation. As the thermal conditions at the base of the Schladminger glacier are not yet known, this question cannot be definitively clarified and further research is needed

According to Magnin et al. (2017), statements regarding permafrost degradation (or aggradation) can only be made in combination with a time period. The authors simulated the long-term temperature evolution at three sites with different topographical settings between 3160 and 4300 m in the Mont Blanc massif, from the Little Ice Age (LIA) steady-state conditions to 2100. The simulation model was evaluated with borehole temperature and ERT measurements. Magnin et al. (2017) conclude that permafrost degradation has been progressing since the LIA. Results of their simulations clearly suggest that climate change between the LIA termination and the 2010s, especially since the 1990s, have triggered a permafrost degradation in rockwalls, regardless of which period after the LIA is used for analysis. The higher parts of the vertical ERT profiles have been presumable ice free at least since the onset of the Postglacial as judged from general glacier evolution during the Holocene in the Eastern Alps (Wirsig et al., 2016). Thus, permafrost resulting from significantly different conditions than the lower parts. The lower parts of the rockwall have been ice free for a shorter period of time; hence the time of permafrost formation after the Holocene was shorter and resulted in smaller warmer permafrost layers in the rockwall and respective lower resistivities.

Based on the results of Magnin (et al., 2017) it can be assumed that an aggradation of permafrost after 1850 (with the exception of short cold periods) is rather unlikely and thus permafrost already existed under the glacier ice. However, it is assumed that permafrost is currently degrading in rockwalls. As further changes in the shallow subsurface might become apparent after some years of observation, repeated measurements might clarify the question of degradation or aggradation of permafrost.

6 Conclusions and Outlook

The used methods have proven their applicability for permafrost mapping. For the first time, map indication locations where permafrost is most likely absent or present based on point and profile data is available for the Dachstein area heavily used by tourism. Permafrost was mainly found at cold north exposed rockwalls. At south exposed rockwalls permafrost is expected at higher (2700 m a.s.l.) elevated and colder cold conditions only.

The ERT data are of high quality. The resistivity calibration by using data of a small scale ERT monitoring system proved to be a helpful method to delimit frozen from unfrozen rock.

Since an aggradation of permafrost after 1850 is rather unlikely, permafrost already existed under the glacier ice and is now degrading due to the direct complying to the atmosphere. It seems that local glacier-related landforms like the blow-out depression located at the footslope of the Dirndl mountain ridge are favorable for permafrost.

Permafrost preservation, in very favourable cold conditions at shadowed higher elevations is still possible at Dachstein area with MAAT below -2.5 °C (2013), but already north, northwest as well as northeast exposed rockwalls show temperature related degradation effects with very heterogeneous (between frozen and unfrozen parts) subsurface ERT tomograms.



Continuous future permafrost monitoring is intended using data from the rather new permafrost borehole in the study area (Schnepfleitner et al., 2015). However, so far the borehole caused many problems and delivered only short data series. After solving this problems, we expect more quantitative information about active layer changes and possible subsurface temperature increase in the future.

5 7 Acknowledgements

This study was supported by the project ‘ROCKING ALPS – Rockfall and Weathering in the Eastern Alps’ financed by the Austrian Science Fund (FWF) through project no. FWF: P24244. Further thanks to the following organisations: Dachstein cable car company (E. Schnepfleitner and L. Traninger), Austrian Federal Forests, "snowreporter" for private climate and snow depth data, as well to G. K. Lieb for fruitful discussions. Many thanks to Johannes Stangl, Eric Rascher, Reinhold
10 Schöngrundner, Patrick Zinner and Eduard Rode for their help during fieldwork.

8 References

- Angelopoulos, M., Pollard, W.H., Couture, N.: The application of CCR and GPR to characterize ground ice conditions at Parsons Lake, Northwest Territories. *Cold Regions Science and Technology* 85: 22-33, 2013.
- Benn, D.I., Evans, D.J.A.: *Glaciers and Glaciation – Second Edition*. Hodder Arnold Publication, 802 pp, 2010.
- 15 – Boeckli, L., Brenning, A., Gruber, S., Noetzli, J.: A statistical approach to modelling permafrost distribution in the European Alps or similar mountain ranges. – In: *The Cryosphere* 6 (1), S. 125–140, 2012a.
- Boeckli, L., Brenning, A., Gruber, S. and Noetzli, J.: Permafrost distribution in the European Alps: calculation and evaluation of an index map and summary statistics. – In: *The Cryosphere* 6, 807–820, 2012b.
- Brenning A., Gruber S. & Hoelzle M.: Sampling and statistical analyses of BTS measurements. *Permafrost and*
20 *Periglacial Processes* 16: 383–393, 2005.
- Draebing, D., Haberkorn, A., Krautblatter, M., Kenner, R. and Phillips M.: Thermal and mechanical responses resulting from spatial and temporal snow cover variability in permafrost rock slopes. *Permafrost and Periglacial Processes* 28 (1):140-157, 2017a.
- Draebing, D., Krautblatter, M. and Hoffmann T.: Thermo-cryogenic controls of fracture kinematics in permafrost
25 rockwalls. *Geophysical Research Letters* 44: 3535-3544, 2017b.
- Ebohon, B. and Schrott, L.: Modeling Mountain Permafrost Distribution. A New Permafrost Map of Austria. – In: Kane, D. und Hinkel, K. (ed.), *Proceedings of the Ninth International Conference on Permafrost, Fairbanks, Alaska*, 397–402, 2009.
- Fischer, A., Seiser, B., Stocker-Waldhuber, M., Mitterer, C., Abermann, J.: Tracing glacier changes in Austria from the
30 Little Ice Age to the present using a lidar-based high-resolution glacier inventory in Austria. *The Cryosphere*, 9(2), 753-766, doi:10.5194/tc-9-753-2015, 2015.
- Frauenfelder, R.: *Regional-scale modelling of the occurrence and dynamics of rockglaciers and the distribution of paleopermafrost*, Schriftenreihe Physische Geographie, Glaziologie und Geomorphodynamik, University of Zurich, 2005.
- Gasser, D., Gusterhuber J., Krische, O., Pühr, B., Scheucher, L., Wagner T. and Stüwe K.: *Geology of Styria: An Overview: Mitteilungen des Naturwissenschaftlichen Vereines für Steiermark*, 139, 5–36, 2009.
- GBA - Geologische Bundesanstalt: *Geologischen Karte der Republik Österreich*, Bl. 96 Bad Ischl, Wien, 1982.



- Gobiet, A., Kotlarski, S., Beniston, M., Heinrich, G., Rajczak J. and Stoffel M.: 21st century climate change in the European Alps-A review. *Sci. Total Environ.*, 493, 1138-1151, doi: 10.1016/j.scitotenv. 2013.07.050., 2014.
- Gruber, S., Peter, M. and Hoelzle, M.: Surface temperatures in steep Alpine rock faces—A strategy for regional-scale measurement and modelling, *Proc. 8th Int. Conf. Permafrost*, 1, 325– 330, 2003.
- 5 – Gubler, S., Fiddes J., Keller, M., and Gruber S.: Scale-dependent measurement and analysis of ground surface temperature variability in alpine terrain. *The Cryosphere*, 5, 431-443, 2011.
- Haeberli, W.: Die Basis-Temperatur der winterlichen Schneedecke als möglicher Indikator für die Verbreitung von Permafrost in den Alpen. – In: *Zeitschrift für Gletscherkunde und Glazialgeologie* 9 (1-2), 221–227, 1973.
- Haeberli, W.: Untersuchungen zur Verbreitung von Permafrost zwischen Flüelapass und Piz Grialetsch (Graubünden).
10 *Mitteilungen der Versuchsanstalt für Wasserbau, Hydrologie u. Glaziologie der ETH Zürich*, 17, Zürich, 221, 1975.
- Haeberli, W., Hoelzle, M.: Application of inventory data for estimating characteristics of and regional climate-change effects on mountain glaciers: a pilot study with the European Alps. *Annals of Glaciology*, 21, 206-212, 1995.
- Haeberli, W., Wegmann, M. and Vonder Mühl D.: Slope stability problems related to glacier shrinkage and permafrost degradation in the Alps, *Eclogae Geol. Helv.*, 90, 407– 414, 1997.
- 15 – Haeberli W., Hoelzle M., Paul F. and Zemp M.: Integrated monitoring of mountain glaciers as key indicators of global climate change: the European Alps. *Annals of Glaciology* 46, 150-160, 2007.
- Haeberli W., Huggel C., Paul F. & Zemp M.: Glacial responses to climate change. In: *Treatise on Geomorphology*, 13, Academic Press, San Diego: p. 152-175, 2013.
- Hartmeyer, I., Keuschnig, M., and Schrott, L.: Long-term monitoring of permafrost-affected rock faces – A scale-oriented
20 approach for the investigation of ground thermal conditions in alpine terrain, Kitzsteinhorn, Austria. *Austrian Journal of Earth Science*, 105 (2): 128–139, 2012.
- Harris, C., Davies, M., and Etzelmüller, B.: The assessment of potential geotechnical hazards associated with mountain permafrost in a warming global climate, *Permafrost and Periglacial Processes*, 12, 145–156, 2001.
- Harris, C., Vonder Mühl, C., Isaksen, K., Haeberli, W., Sollid, J. L., King, L., Holmlund, P., Dramis, F., Gugliemin, M.,
25 and Palacios, D.: Warming permafrost in European mountains, *Global and Planetary Change*, 39, 215–225, 2003.
- Hauck, C.: Geophysical methods for detecting permafrost in high mountains, 171, *ETH Zurich, Zurich*, 1–204, 2001.
- Hauck, C., Vonder Mühl, D. and Maurer H.: Using DC resistivity tomography to detect and characterize mountain permafrost. *Geophysical Prospecting* 51:273–284, 2003.
- Hauck, C. and Kneisel, C.: *Applied Geophysics in Periglacial Environments*, University Press, Cambridge, 240 pp., 2008.
- 30 – Helfricht, K.: Veränderungen des Massenhaushaltes am Hallstätter Gletscher seit 1856. – Diplomarbeit, Institut für Meteorologie und Geophysik. *Leopold-Franzens-Universität Innsbruck*, 139, 2009.
- Hilbich, C., Marescot, L., Hauck, C., Loke, M.H. and Mäusbacher, R.: Applicability of Electrical Resistivity Tomography Monitoring to coarse blocky and ice-rich permafrost landforms. *Permafrost and Periglacial Processes* 20(3): 269–284. DOI: 10.1002/ppp.652, 2009.
- 35 – Humlum O.: The climatic significance of rock glaciers. *Permafrost and Periglacial Processes* 9: 375-395, 1998.
- Ishikawa, M.: Thermal regimes at the snow–ground interface and their implications for permafrost investigation. – In: *Geomorphology* 52 (1–2), S. 105–120, 2003.
- Kellerer-Pirklbauer, A.: A regional signal of significant recent ground surface temperature warming in the periglacial environment of Central Austria. In: Günther, F., Morgenstern, A. (Eds.), *XI. International Conference On Permafrost –
40 Book of Abstracts*, 20–24 June 2016. Bibliothek Wissenschaftspark Albert Einstein, Potsdam, Germany, pp. 1025–1026, 2016.



- Kellerer-Pirklbauer A.: Potential weathering by freeze-thaw action in alpine rocks in the European Alps during a nine year monitoring period. *Geomorphology* 296 (2017) 113–131. <http://dx.doi.org/10.1016/j.geomorph.2017.08.020>, 2017.
- Kellerer-Pirklbauer A., Lieb G.K., Avian M. & Carrivick J.: Climate change and rock fall events in high mountain areas: Numerous and extensive rock falls in 2007 at Mittlerer Burgstall, Central Austria. *Geografiska Annaler: Series A, Physical Geography*, 94, 59-78, 2012.
- Kellerer-Pirklbauer, A., Lieb, G., Avian, M. and Gspurning J.: The Response of Partially Debris-Covered Valley Glaciers to Climate Change: The Example of the Pasterze Glacier (Austria) in the Period 1964 to 2006. *Geografiska Annaler. Series A, Physical Geography*, 90, 4, 269-285, 2008.
- Kern K., Lieb G.K., Seier G. & Kellerer-Pirklbauer A.: Modelling geomorphological hazards to assess the vulnerability of alpine infrastructure: The example of the Großglockner-Pasterze area, Austria. *Austrian Journal of Earth Sciences*, 105/2, 113-127, 2012.
- Kneisel, C., Hauck, C., Fortier, R., and Moonman, B.: Advances in geophysical methods for permafrost investigations, *Permafrost Periglac.*, 19, 157–178, doi:10.1002/ppp.616, 2008.
- Knödel, K., Krummel H., and Lange, G. (ed.): *Geophysik Handbuch zur Erkundung des Untergrundes von Deponien und Altlasten*. Springer Verlag, Berlin, Band 3, 1102, 2005.
- Krautblatter, M. and Hauck, C.: Electrical resistivity tomography monitoring of permafrost in solid rockwalls, *J. Geophys. Res.- Earth*, 112, F02S20, doi:10.1029/2006jf000546, 2007.
- Krautblatter, M., Funk, D. and Günzel F.: Why permafrost rocks become unstable: a rock–ice-mechanical model in time and space. *Earth Surface Processes and Landforms*, 38, 8, 876–887, 2013.
- Krautblatter, M., Verleysdonk, S., Flores-Orozco, A., and Kemna, A.: Temperature-calibrated imaging of seasonal changes in permafrost rockwalls by quantitative electrical resistivity tomography (Zugspitze, German/Austrian Alps), *J. Geophys. Res.-Earth*, 115, F02003, doi:10.1029/2008JF001209, 2010.
- Krobath, M. and Lieb, G.: Die Dachsteingletscher im 20. Jahrhundert. – In: Brunner, K. (ed.), *Das Karls-Eisfeld. Forschungsarbeiten am Hallstätter Gletscher. Wissenschaftliche Alpenvereinshefte, H. 38, Haus des Alpinismus, München*, 75–101, 2004.
- Laxton, S. and Coates, J.: Geophysical and borehole investigations of permafrost conditions associated with compromised infrastructure in Dawson and Ross River, Yukon. *In: Yukon Exploration and Geology 2010*, K.E. MacFarlane, L.H. Weston and C. Relf (eds.), Yukon Geological Survey, 135-148, 2011.
- Lieb, G. and Schopper, A.: Zur Verbreitung von Permafrost am Dachstein (Nördliche Kalkalpen, Steiermark). – In: *Mitt. naturwiss. Ver. Steiermark* 121, 149–163, 1991.
- Lieb, G., Kellerer-Pirklbauer, A., Strasser U.: Effekte des Klimawandels im Naturraum des Hochgebirges. In: Fassmann H. and Glade T. (eds) (Hg.): *Geographie für eine Welt im Wandel – 57. Deutscher Geographentag 2009 in Wien*. 2012.
- Loke, M.H.: *Electrical imaging surveys for environmental and engineering studies, a practical guide to 2-D and 3-D surveys*. Copyright by M.H. Loke, Penang (Malaysia), 1999.
- Magnin, F., Josnin J., Ravanel L., Pergaud J., Pohl B., and Deline P.: Modelling rock wall permafrost degradation in the Mont Blanc massif from the LIA to the end of the 21st century. *The Cryosphere* 11, 1813–1834, 2017.
- Magnin, F., Krautblatter, M., Deline, P., Ravanel, L., Malet E. and Bevington, A.: Determination of warm, sensitive permafrost areas in near-vertical rockwalls and evaluation of distributed models by electrical resistivity tomography. *Journal of Geophysical Research* 120, 5, 745–762, 2015. 10.1002/2014JF003351, 2015.



- Marescot, L., Loke, M.H., Chapellier, D., Delaloye, R., Lambiel, C. and Reynard, E.: Assessing reliability of 2D resistivity imaging in permafrost and rock glacier studies using the depth of investigation index method. *Near Surface Geophysics* 1(2): 57–67, 2003.
- Matsuoka, N. and Murton, J.: Frost weathering: Recent advances and future directions, *Permafrost Periglac.*, 19, 195-210, 5 2008.
- Matsuoka, N. and Sakai H.: Rockfall activity from an alpine cliff during thawing periods. *Geomorphology*, 28, 3-4, 309-328, 1999. doi:10.1016/S0169-555X(98)00116-0, 1999.
- Moser, R.: *Dachsteingletscher und deren Spuren im Vorfeld*, Musealverein Hallstatt, Hallstatt, 143, 1997.
- Österreichischer Alpenverein: *Jahrbuch des Österreichischen Alpenvereins (Alpenvereinszeitschrift)*. Bd. 83, 10 Universitätsverlag Wagner, Innsbruck, 158 S., 1958.
- Oldenburg, D.W. and Li, Y.G.: Estimating depth of investigation in dc resistivity and IP surveys. *Geophysics* 64(2): 403–416. DOI: 10.1190/1.1444545, 1999.
- Otto, J and Keuschnig, M.: *Permafrost-Glacier Interaction – Process Understanding of Permafrost Reformation and Degradation*. Austrian Permafrost Research Initiative. Final Report, Chapter: 1, Publisher: ÖAW - Austrian Academy of 15 Sciences, Editors: Martin Rutzinger, Kati Heinrich, Axel Borsdorf, Johann Stötter, 3-16, 2014.
- Paul, F., Kääh, A., Maisch, M., Kellenberger, T. W., and Haerberli, W.: Rapid disintegration of Alpine glaciers observed with satellite data, *Geophys. Res. Lett.*, 31, L21402, doi:10.1029/2004GL020816, 2004.
- Raveland, L. And Deline P.: Climate influence on rockfalls in high-Alpine steep rockwalls: The north side of the Aiguilles de Chamonix (Mont Blanc massif) since the end of the ‘Little Ice Age’. *The Holocene* 21, 2, 357-365. doi: 20 10.1177/0959683610374887, 2011.
- Rödder, T. and Kneissel, C.: Permafrost mapping using quasi-3D resistivity imaging, Murtèl, Swiss Alps. *Near Surface Geophysics*, 10, 2, 117 – 127, 2012.
- Sattler, K., Keiler, M., Zischg, A., and Schrott, L.: On the Connection between Debris Flow Activity and Permafrost Degradation: A Case Study from the Schnalstal, South Tyrolean Alps, Italy. *Permafrost and Periglacial Processes*, 22 (3): 25 254-265, 2011.
- Schmid, M., Gubler, S., Fiddes, J. and Gruber, S.: Inferring snowpack ripening and melt-out from distributed measurements of near-surface ground temperatures. – In: *The Cryosphere* 6 (5), S. 1127-1139, 2012.
- Schnepfleitner, H., Kellerer-Pirklbauer, A., Rode M.: The permafrost borehole “Koppenkarstein North Face”, Dachstein Massif: An Austrian contribution to the Global Terrestrial Network for Permafrost (GTN-P), *Joannea Geologie und 30 Paläontologie* 12: 28-36, 2016.
- Schopper, A.: *Die glaziale und spätglaziale Landschaftsgenese im südlichen Dachstein und ihre Beziehung zum Kulturlandausbau*. – Diplomarbeit. Karl-Franzens- Universität Graz, 161, 1989.
- Schrott, L. and Sass, O.: Application of field geophysics in geomorphology: Advances and limitations exemplified by case studies. – In: *Geomorphology* 93: 55-73, 2008.
- 35 – Simony, F.: *Photographische Aufnahmen und Gletscheruntersuchungen im Dachsteingebirge*. – In: *Mitteilungen des Deutschen und Österreichischen Alpenvereins*, 10, S. 314-317, 1884.
- Simony, F.: *Das Dachsteingebiet. Ein geographisches Charakterbild aus den Österreichischen Nordalpen*, Hölzel, Wien, 152, 1895.
- snowreporter (2013): *snowreporter Telekommunikationssysteme GmbH, Klimadatensatz Dachstein*, Graz. – E-Mail, 40 10/2013.



- Stiegler, C., Rode, M., Sass, O. and Otto, J.: An Undercooled Scree Slope Detected by Geophysical Investigations in Sporadic Permafrost below 1000 M ASL, Central Austria. *Earth Surface Processes*, 25, 3, 194–207, 2014.
- Supper, R., Ottowitz, D., Jochum, B., Römer, A., Pfeiler, S., Kauer, S., Keuschnig, M. and Ita, A.: Geoelectrical monitoring of frozen ground and permafrost in alpine areas: field studies and considerations towards an improved measuring technology, *Near Surface Geophysics*, 2014, 12, 93-115, 2014.
- 5 – Suter, S., Laternser, M., Haeberli, W., Frauenfelder R. and Hoelzle, M.: Cold firn and ice of high altitude glaciers in the Alps: measurements and distribution modelling *Journal of Glaciology*, 47 (156): 85–96, 2001.
- Wakonigg, H.: *Witterung und Klima in der Steiermark*, Verlag für die technische Universität Graz, Graz, 473, 1978.
- Wegmann, M., Gudmundsson G. and Haeberli, W.: Permafrost changes and the retreat of Alpine glaciers: A thermal modelling approach, *Permafrost Periglacial Processes*, 9, 23–33, 1998.
- 10 – Wirsig C., Zasadni J., Christl M., Akçar N., Ivy-Ochs S.: Dating the onset of LGM ice surface lowering in the High Alps, *Quaternary Science Reviews*, 143 (2016) 37-50, 2016.
- Zemp, M., Paul, F., Hoelzle, M., and Haeberli, W.: Glacier fluctuations in the European Alps 1850–2000: an overview and spatiotemporal analysis of available data, in: *The darkening peaks: Glacial retreat in scientific and social context*, edited by: Orlove, B., Wiegandt, E., and Luckman, B., University of California Press, in press, 2006.
- 15